

1 **The influence of environmental setting on the community ecology of Ediacaran organisms**

2

3 *Emily G. Mitchell*¹, *Nikolai Bobkov*^{2,3}, *Natalia Bykova*^{2,4}, *Alavya Dhungana*⁵, *Anton*

4 *Kolesnikov*^{2,6,7}, *Ian R. P. Hogarth*^{8,9}, *Alexander G. Liu*¹⁰, *Tom M.R. Mustill*^{10,11}, *Nikita*

5 *Sozonov*^{2,3}, *Shuhai Xiao*⁴ and *Dmitriy V. Grazhdankin*^{2,3}.

6

7 ek338@cam.ac.uk

8

9 ¹Department of Zoology, University of Cambridge, UK.

10 ²Institute of Petroleum Geology and Geophysics, Novosibirsk, Russian Federation.

11 ³Novosibirsk State University, Russian Federation.

12 ⁴Department of Geosciences, Virginia Tech, Blacksburg, VA 24061, United States.

13 ⁵Department of Earth Sciences, Durham University, UK.

14 ⁶Geological Institute, Russian Academy of Sciences, Moscow, Russian Federation.

15 ⁷Department of Geography, Moscow Pedagogical State University, Moscow, Russian
16 Federation.

17 ⁸Department of Chemical Engineering, University of Cambridge, UK.

18 ⁹Current address: University College London, UCL Institute for Innovation and Public
19 Purpose, UK.

20 ¹⁰Department of Earth Sciences, University of Cambridge, UK.

21 ¹¹Current address: Gripping Films, St. John's Church Road, London, England, E9 6EJ.

22

23

24

25 **Abstract**

26 The broad-scale environment plays a substantial role in shaping modern marine ecosystems,
27 but the degree to which palaeocommunities were influenced by their environment is unclear.
28 To investigate how broad-scale environment influenced the community ecology of early
29 animal ecosystems we employed spatial point process analyses to examine the community
30 structure of seven bedding-plane assemblages of late Ediacaran age (558–550 Ma), drawn from
31 a range of environmental settings and global localities. The studied palaeocommunities exhibit
32 marked differences in the response of their component taxa to sub-metre-scale habitat
33 heterogeneities on the seafloor. Shallow-marine palaeocommunities were heavily influenced
34 by local habitat heterogeneities, in contrast to their deep-water counterparts. Lower species
35 richness in deep-water Ediacaran assemblages compared to shallow-water counterparts across
36 the studied time-interval could have been driven by this environmental patchiness, because
37 habitat heterogeneities correspond to higher diversity in modern marine environments. The
38 presence of grazers and detritivores within shallow-water communities may have promoted
39 local patchiness, potentially initiating a chain of increasing heterogeneity of benthic
40 communities from shallow to deep-marine depositional environments. Our results provide
41 quantitative support for the “Savannah” hypothesis for early animal diversification – whereby
42 Ediacaran diversification was driven by patchiness in the local benthic environment.

43

44 **Keywords**

45 Ediacaran, palaeoecology, spatial analysis, early animal diversification.

46 **Author Contributions**

47 E. Mitchell conceived this paper and wrote the first draft. N. Bobkov, A. Kolesnikov, N.
48 Sozonov and D. Grazhdankin collected the data for DS surface. N. Bobkov and N. Sozonov
49 performed the analyses on DS surface. N. Bykova, S. Xiao, and D. Grazhdankin collected the

50 data for WS, KH1 and KH2 surfaces and E. Mitchell performed the analyses. A. Dhungana
51 and A. Liu collected the data for FUN4 and FUN5 surfaces and A. Dhungana performed the
52 analyses. T. Mustill and D. Grazhdankin collected the data for KS and T. Mustill and E.
53 Mitchell performed the analyses. I. Hogarth developed the software for preliminary KS surface
54 analyses. E. Mitchell, N. Bobkov, N. Bykova, A. Dhungana, A. Kolesnikov, A. Liu, S. Xiao
55 and D. Grazhdankin discussed the results and prepared the manuscript.

56

57 **Background**

58 The Ediacaran–Cambrian transition (~580–520 million years ago) is one of the most
59 remarkable intervals in the history of life on Earth, witnessing the rise of large, complex
60 animals in the global oceans (1,2). The diversification of early animals coincides with dramatic
61 perturbations in the global abiotic environment, including changes to carbon cycling and a
62 progressive but dynamic oxygenation of the oceans (3,4). The extent to which animals
63 themselves drove these global changes is a matter of considerable debate (5–7) with several
64 competing hypotheses suggested to explain their observed diversification. These include global
65 abiotic changes that occurred over kilometre scales (8,9) and biotic factors acting over local
66 scales (metre to kilometre), and include organism interactions such as burrowing and/or
67 predation (10,11). Feedbacks between biotic and abiotic factors have also been proposed as
68 drivers of early animal diversification, whereby Ediacaran organisms directly or indirectly
69 created patchy food resources, stimulating the evolution of mobile bilaterians (12,13). Due to
70 the small (within community) spatial scales over which key evolutionary mechanisms often act
71 (14), investigation of the community ecology of Ediacaran assemblages over broad (kilometre)
72 spatial scales offers an opportunity to link the interactions of individual organisms to macro-
73 evolutionary and macro-ecological trends. In this study, we investigate the relationship
74 between late Ediacaran early animal diversification and the broad-scale environment.

75

76 Ediacaran macrofossils occur globally across a wide-range of palaeo-environments (1).

77 Previous studies have separated late Ediacaran palaeocommunities into three taxonomically

78 distinct assemblages – the Avalon, White Sea and Nama – which occupy partially overlapping

79 temporal intervals and different water-depths with no significant litho-taphonomic or

80 biogeographic influence (15–17). This study focusses on palaeocommunities within the

81 Avalon and White Sea fossil assemblages that are considered to reflect original in situ

82 communities (18,19), permitting the use of statistical analyses of the distribution of fossil

83 specimens on bedding planes (spatial point process analyses, SPPA) to reconstruct the

84 interaction of organisms with each other and their local environment (20–25). The Avalon

85 assemblage is primarily represented by sites in Newfoundland, Canada and Charnwood Forest

86 UK (26,27), and typically documents mid-shelf/deep-water settings (from depths below the

87 edge of the continental shelf – the slope break) of 575–566 Ma (28,29). Such sites exhibit

88 relatively limited ecological and morphological diversity (30,31), and palaeocommunities

89 consisting almost exclusively of sessile taxa (32) that show only weak trends with community

90 composition along regional palaeoenvironment gradients (20). Previous spatial analyses of

91 Avalonian communities have found limited evidence for environmental interactions within

92 these communities (21–23), in contrast to the strong imprint exerted by resource-limitation on

93 modern deep-sea ecosystems (33,34).

94 Palaeocommunities from the White Sea assemblage are most famously represented by sites in

95 South Australia, and the East European Platform of Russia, dating to ~558–555 Ma (35–37).

96 These assemblages typically document shallow-water, diverse communities including taxa

97 interpreted as bilaterians (38), herbivores (39), detritivores (40) and motile organisms (41).

98 Within the White Sea assemblages, community composition is strongly correlated with

99 sedimentary environment and the presence of textured organic surfaces at bed-scale level
100 (42,43).

101

102 Metrics of taxonomic and ecological diversity are much higher in White Sea assemblages than
103 in Avalonian ones, with changes in taxonomic and morphological diversity calculated to be of
104 similar magnitude to those between the Ediacaran and Cambrian (30,31). These Ediacaran
105 assemblages have high beta-diversity compared to modern benthic systems (44), but the
106 driving processes underlying this high diversity are not understood. The regional
107 palaeoenvironment (kilometre scale) (15,17) has a significant influence on (non-algal
108 dominated) Ediacaran fossil assemblage composition, but metrics influence on local (metre to
109 sub-metre scale) community ecology has not yet been investigated. In modern benthic
110 communities, small spatial scale (< 50 cm) substrate heterogeneities (e.g. substrate variations
111 in nutrients, oxygen patchiness, or biotic and abiotic gradients within microbial mats) exert a
112 significant influence on community ecology (33,34,45). For Ediacaran palaeocommunities, it
113 is not possible from spatial analyses alone to determine the underlying causes of habitat
114 heterogeneities, nor the extent to which they relate to food resources, such as those resulting
115 from the decay of Ediacaran organisms (12,46). However, it is possible to compare how the
116 relative influence of such heterogeneities changes with broad-scale environmental setting:
117 previous analyses have identified assemblage-level trends between community compositions
118 and bathymetric depth (15–17). In this study, we compare the drivers of community ecology
119 between shallow and deep-water Ediacaran palaeocommunities (above or below the slope
120 break) over a ~7-million-year period using spatial analyses of seven palaeocommunities.

121

122 **Spatial analyses**

123 Determining the nature of interactions between fossilised organisms and their environment can
124 be undertaken if entire palaeocommunities are preserved in-situ, such that the position of the
125 fossils on bedding planes can be interpreted to reflect aspects of the organism's life-history
126 (47). For sessile organisms, such as in the Avalon communities, community-scale spatial
127 distributions are dependent upon the interplay of a limited number of factors: physical
128 environment (which manifests as habitat associations of a taxon or taxon-pairs (48)); organism
129 dispersal/reproduction (49); competition for resources (50); facilitation between taxa (where
130 one taxon increases the survival another taxa) (51); and differential mortality (52). For fossil
131 assemblages containing mobile taxa (e.g. the White Sea assemblages), behavioural ecology
132 also influences spatial distributions, so interpretations of their spatial distributions are
133 qualitative rather than quantitative.

134

135 Studies of modern ecosystems have demonstrated that habitat associations resulting from
136 interactions between organisms and their local environment can be either positive, leading to
137 aggregations of individuals (such as around a preferential substrate for establishment), or
138 negative segregation away from such patches (21). SPPA are a suite of analyses compare the
139 relative density of points (in this case fossil specimens) to different models corresponding to
140 different ecological processes, in order to infer the most likely underlying process responsible
141 for producing the observed spatial distribution. For sessile organisms, habitat associations
142 identified by SPPA are best-modelled by a heterogeneous Poisson model (HP), or when
143 combined with dispersal limitations, an Inhomogeneous Thomas Cluster model (ITC) (53,54).
144 Where the local environment is resource-limited to the extent that it significantly reduces
145 organism densities, this is indicated by spatial segregation between specimens within a
146 community (55). When sessile populations are not significantly affected by their local
147 environment, their spatial distributions are completely spatially random (CSR), indicating no

148 significant influence by any biological or ecological processes at the spatial scale investigated,
149 or alternatively reflect dispersal/reproductive processes (48,54,56–58). CSR is modelled by
150 homogeneous Poisson processes (47), whereas dispersal patterns are best modelled by best-fit
151 Thomas Cluster (TC) or Double Thomas Cluster (DTC) models (54). Facilitation (where one
152 taxa increases the survival of another) is best-modelled by linked-cluster models (51,59) and
153 density-dependent processes detected using random-labeling analyses (52,60).

154

155 **Geological setting**

156 We assessed the community palaeoecology of seven fossil-bearing assemblages across five
157 different global Ediacaran locations, spanning the full range of known habitats inhabited by
158 members of the Ediacaran macrobiota during the late Ediacaran interval, and incorporated data
159 from previous studies (21,23) on Avalonian palaeocommunities for comparison. These
160 localities document a range of diverse local depositional environments, but in order to focus
161 on the broadest macro-ecological and macro-evolutionary patterns we have coarsely grouped
162 them within either shallow or deep-water settings.

163

164 *Shallow marine settings*

165 Five of the studied palaeocommunities are found in facies that reflect shallow marine depositional
166 environments. Palaeocommunity WS is an *Aspidella*-bearing surface on the underside of a wave-
167 rippled sandstone within a thick package of mudstones and sandstones deposited in a prograding,
168 storm-influenced depositional system (61,62). It was collected from the Lyamtsa Formation of the
169 Valdai Group, along the Onega Coast of the White Sea, Russian Federation, and remained in the field
170 where it was destroyed by landslides. *Aspidella* specimens were collected and are stored uncatalogued
171 at the Trofimuk Institute for Petroleum Geology and Geophysics in Novosibirsk. The Lyamtsa
172 Formation is older than a date of 558 ± 1 Ma (U/Pb zircon dating of volcanic tuffs near the base of the

173 overlying Verkhovka Formation) (16). Surface (KS) is on the lower surface of a finely laminated
174 sandstone, interpreted as a flood deposit within a prograding prodelta depositional system (63). This
175 surface, within the lower member of the Erga Formation (Winter Coast of the White Sea) (16,35),
176 contains the fossil *Kimberella*, and is younger than 552.85 ± 0.77 Ma (64) (date recalculated from
177 Martin et al. (65)). The KS surface remained in the field and has been subsequently destroyed by land
178 slides and weathering. Two *Funisia*-bearing surfaces from the base of thin-bedded wave-rippled
179 quartz sandstones representing deposition in prodelta marine settings between fair-weather and storm
180 wave base originate from the Ediacara Member of South Australia (42,66–68). These surfaces reside
181 in the collections of the South Australia Museum, with surface FUN4 collected from Ediacara
182 Conservation Park (SAM P55236) and surface FUN5 collected from the Mount Scott Range (SAM
183 P41506). Since FUN4 and FUN5 originate from different localities (> 50 km apart), it is assumed
184 likely that they represent discrete bedding plane/palaeocommunities. The South Australian Ediacaran
185 successions have not been radiometrically dated, but the Ediacara Member is widely assumed to be of
186 a similar age to the White Sea fossil-bearing sections (1,2).

187

188 Surface DS is a *Dickinsonia*-bearing surface from the Konovalovka Member of the Cherny
189 Kamen Formation, cropping out along the Sylvitsa River, Central Urals, Russia (63,69). It
190 lies within an interval of finely alternating wave-rippled sandstones, siltstones and mudstones
191 that are sandwiched between two thick intervals of biolaminated sandstone characterised by
192 microbial shrinkage cracks and salt crystal pseudomorphs (70). The overall succession is
193 considered transitional from marginal marine to non-marine, with the fossil-bearing interval
194 interpreted as having been deposited in a lagoon within a tidal flat depositional system (70).
195 A U/Pb zircon date of 557 ± 13 Ma from volcanic tuffs near the base of the Cherny Kamen
196 Formation (63) suggests that this unit may have been deposited broadly coevally with those
197 on the White Sea coast. Specimens from this surface reside in Novosibirsk State University,

198 Russian Federation (specimen numbers: 2057-001 to 2057-003) and will be placed at the Ural
199 Geological Museum (Yekaterinburg).

200

201 All five of these surfaces therefore represent siliciclastic depositional environments from
202 above the slope break, and so fall broadly into the grouping of “shallow marine”. They
203 contain examples of taxa interpreted as animals (e.g. *Dickinsonia*, *Kimberella*) as well as
204 non-metazoans (*Orbisiana*) and their age and facies place them within the White Sea
205 assemblage (15,17).

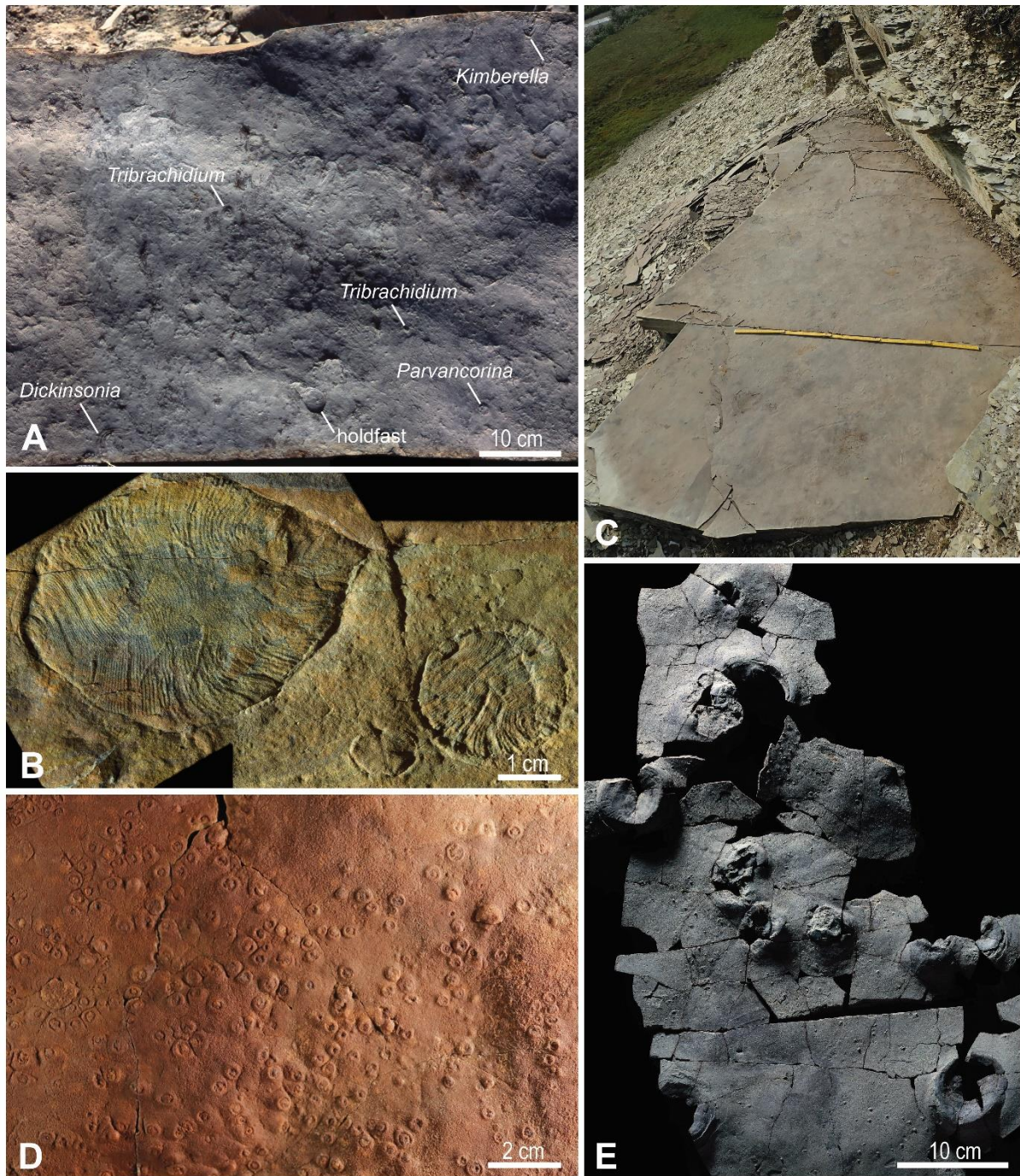
206

207 *Deep-water marine setting*

208 Two bedding surfaces dominated by *Aspidella* specimens (KH1 and KH2) were collected
209 from a package of finely alternating limestone and shale interbeds within the Khatyspyt
210 Formation, Olenek River, Siberia. Sedimentological observations (e.g., turbiditic nature of
211 the limestones; evidence of strong unidirectional flows; intraclasts originating from outside of
212 the Khatyspyt depositional basin) suggest the Khatyspyt Formation was deposited within a
213 starved intracratonic rift basin developed in a marine ramp setting within a relatively deep-
214 water setting beyond the shelf slope break (71–74). A positive $\delta^{13}\text{C}_{\text{carb}}$ excursion in the
215 Khatyspyt Formation has been correlated with an excursion of similar magnitude in the <550
216 Ma Gaojiashan Member of the Dengying Formation (74). Strontium isotope ratios ($^{87}\text{Sr}/^{86}\text{Sr}$)
217 in the Khatyspyt Formation are consistently ca. 0.7080 (74,75), a value approaching some of
218 the ratios seen in the Gaojiashan Member (76), so this correlation seems plausible. Surface
219 KH2 remains in the field and surface KH1 was destroyed while excavated KH. Specimens
220 from KH1 surface reside in Trofimuk Institute for Petroleum Geology and Geophysics,
221 collection number 913 (specimen numbers: 0607/2009-3, 0607/2009-6, 0607/2009-7,
222 0607/2009-17, 0607/2009-18).

223

224



225

226 **Fig. 1. Assemblages of Ediacaran fossils from study localities.** A) A fragment of the

227 *Kimberella* surface (KS), indicating key taxa, lower Erga Formation, Winter Coast of the White

228 Sea. B) Specimens of *Dickinsonia* from the *Dickinsonia* surface (DS), Konovalovka Member,

229 Cherny Kamen Formation, Sylvitsa River, Central Urals. C) The *Aspidella* surface (KH1),

230 Khatyspyt Formation, Olenek Uplift, Northern Siberia. Metre rule for scale. D) *Funisia* from
231 FUN4 surface (SAM P55236), Ediacara Member, Rawnsley Quartzite, South Ediacara, Flinders
232 Range, South Australia. E) A representative fragment of the WS surface, upper Lyamtsa
233 Formation, White Sea Region. This particular fragment was not included in the analysis. These
234 data were compared with 7 palaeocommunities that have been subjected to SPPA in previous
235 studies (21,23), where details of data collection and locality information are described.

236

237 **Data Collection**

238 Spatial data were collected from the surfaces using different methods depending on the
239 physical properties of the bedding plane. The WS, KH1, KH2 surfaces were mapped in the
240 field (WS in 2017, KH1 in 2006 and 2009, and KH2 in 2018) onto millimetre graph paper.
241 First, the co-ordinates of the edge of the rock surface were recorded, then the co-ordinates,
242 orientation and dimensions of each of the specimen were measured and plotted onto the paper.
243 For DS, a bedding surface of 9 m² was excavated over the course of two years (2017–2018).
244 The surface was photo-mapped, with photographs taken under an artificial light source at night.
245 The intersection between maximum length (L) and maximum width (W) of each specimen was
246 taken to be the absolute position of the organism, with measurements obtained from digital
247 photographs using Adobe Photoshop CC software and Apple Script Editor.

248

Surface	Environmental setting	Species richness	Dominant Taxa	Specimen numbers	Area mapped (m ²)
WS	Shallow	1	<i>Aspidella</i>	40	0.54
KH1	Deep	2	<i>Aspidella</i>	204	2.38
KH2	Deep	2	<i>Aspidella</i>	81	1.52
DS	Shallow	1	<i>Dickinsonia</i>	62	9.00
KS	Shallow	13	<i>Kimberella</i> , <i>Orbisiana</i>	107	2.74
FUN4	Shallow	2	<i>Funisia</i>	290	0.69
FUN5	Shallow	1	<i>Funisia</i>	482	0.78

249

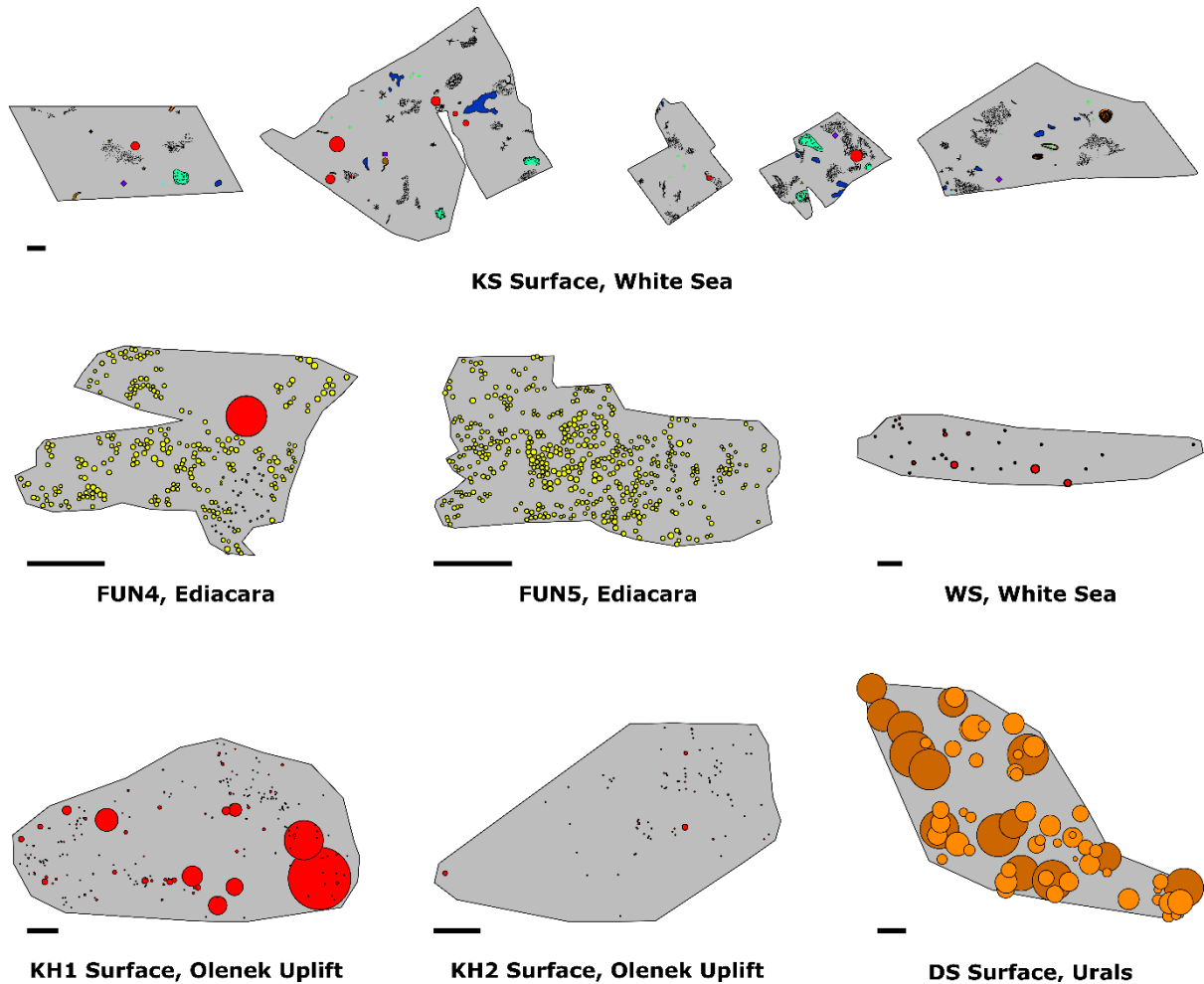
250 **Table 1. Summary data of the surfaces mapped.** The environmental setting, species richness,
251 specimen numbers within the mapped area, and the total mapped area are provided.

252

253 The KS surface was excavated in July 2004, and is a laterally discontinuous transect consisting
254 of four slabs of variable size, ranging from 0.6×0.4 m to 1.6×1.0 m. The relative positions
255 of the slabs within the transect were mapped in situ on an excavated terrace. A separate block
256 originating from the same horizon was found in float close to the transect. Following
257 reassembly, the taxonomic identity, positions, orientations and shapes of the fossils were
258 mapped at millimetre scale. For the FUN4 and FUN5 surfaces, photogrammetric maps of the
259 bedding surfaces were made, with lens edge effects corrected using RawTherapee (v. 2.4.1).
260 For all mapped palaeocommunities, fossil identification, position, and dimensions (disc width,
261 disc length, stem length, stem width, frond length, and frond width) were digitized in Inkscape
262 0.92.3 on a 2D projection of the dataset, resulting in a 2D vector map for each
263 palaeocommunity. Only taxa that had sufficient abundance (> 5 specimens) for spatial analyses
264 were formally identified, and these were grouped within one of six taxonomic groups:
265 *Aspidella*, *Dickinsonia*, *Funisia*, *Kimberella*, *Orbisiana*, and the trace fossil *Kimberichnus*. A
266 group consisting of all the sessile taxa on the KS surface was also assessed, because abundance
267 was not sufficient to include all taxa individually. Analyses were not conducted for individual
268 low abundance taxa whose specimen numbers fell below the threshold for which results would
269 be statistically meaningful.

270

271



272

KH1 Surface, Olenek Uplift

KH2 Surface, Olenek Uplift

DS Surface, Urals

273

Fig 2. Spatial maps of the seven studied palaeocommunities. Scale bar is 10 cm. Different

274

colours indicate different taxa as follows: Red, *Aspidella*; Orange, *Dickinsonia*; Yellow circles,

275

Funisia; Light green scratch marks, *Kimberichnus*; Light green crosses, *Kimberella*; Blue

276

crosses, *Charniodiscus*; Green triangles, *Parvancorina*; Dark blue patches, *Orbisiana*; Black

277

stipples, horizontal traces; White globular strings, *Palaeopasichnus*; Purple diamonds, *Andiva*;

278

Purple squares, *Yorgia*. Size of the circles corresponds to specimen length or diameter (as

279

appropriate). On the DS surface, dark orange circles are the large size-class of *Dickinsonia*,

280

and the light orange represents the small size-class.

281

282

283

284 **Methods**

285 **Bias analyses**

286 For each surface, we first tested for erosional biases and tectonic deformation, since both have
287 the potential to distort spatial analyses (18,73). If these factors were found to have significantly
288 affected specimen density distributions, the erosion and/or deformation were taken into account
289 when performing later analyses (cf. (23)), with heavily eroded sections of the bedding planes
290 excluded from analyses. The influence of tectonic deformation was only observed on the DS
291 surface, so retrodeformation techniques (18,25) were not applied to the spatial maps of WS,
292 KH1, KH2, KS, FUN4 and FUN5 surfaces. Where possible (WS, KH1 and KH2 surfaces), the
293 area near the outcrops was investigated, and no independent evidence for tectonic deformation
294 was found. The holdfast discs on surfaces KS, FUN4 and FUN5 did not show any evidence
295 tectonic deformation. The DS surface showed signs of deformation in the form of consistent
296 variation in specimen length to width ratios along a presumed axis of deformation. The
297 *fitModel* function from the *mosaic* package in R (73) was used to find the best-fit values
298 for the direction and strength of deformation using the assumption that *Dickinsonia* had a
299 consistent length to width ratio during the ontogeny (43,77,78) though note (79)), and the
300 spatial map was retrodeformed cf. (18,23,25).

301

302 **Spatial Analyses**

303 Initial data exploration, inhomogeneous Poisson modelling, and segregation tests were
304 performed in R (75) using the package *spatstat* (80,81). Programita was used to obtain
305 distance measurements and to perform aggregation model fitting (described in detail in
306 references (48,52,80,82–86).

307

308 Univariate and bivariate pair correlation functions (PCFs) were calculated from assemblage
309 population densities using a grid of 1 cm × 1 cm cells on all surfaces except DS, where a 10
310 cm × 10 cm cell size was used to correspond to the larger overall mapped area. To minimise
311 noise, a 3 cell smoothing was calculated dependent on specimen abundance, which was
312 applied to the PCF (59). To test whether the PCF exhibited complete spatial randomness
313 (CSR), 999 simulations were run for each univariate and bivariate distribution, with the 49
314 highest and 49th lowest values removed (59). CSR was modelled by a Poisson model on a
315 homogeneous background where the PCF = 1 and the fit of the fossil data to CSR was
316 assessed using Diggle's goodness-of-fit test (56,87). Note that due to non-independence of
317 spatial data, Monte-Carlo generated simulation envelopes cannot be interpreted as confidence
318 intervals. If the observed data fell below the Monte-Carlo simulations, the bivariate
319 distribution was interpreted to be segregated; above the Monte-Carlo simulations, the
320 bivariate distribution was interpreted to be aggregated (47,59).

321

322 If a taxon was not randomly distributed on a homogeneous background, and was aggregated,
323 the random model on a heterogeneous background was tested by creating a heterogeneous
324 background from the density map of the taxon under consideration. This density map was
325 defined by a circle of radius R over which the density was averaged throughout the sample
326 area. Density maps were formed using estimators within the range of 0.1 m < R < 1 m, with
327 R corresponding to the best-fit model used. If excursions outside the simulation envelopes
328 for both homogeneous and heterogeneous Poisson models remained, then Thomas cluster
329 models were fitted to the data as follows:

330

331 1. The PCF and L-function (88) of the observed data were found. Both measures were
332 calculated to ensure that the best-fit model is not optimized towards only one distance
333 measure, and thus encapsulates all spatial characteristics.

334 2. Best-fit Thomas cluster processes (89) were fitted to the two functions where $PCF > 1$.
335 The best-fit lines were not fitted to fluctuations around the random line of $PCF = 1$ in order
336 to aid good fit about the actual aggregations, and to limit fitting of the model about random
337 fluctuations. Programita used the minimal contrast method (56,87) to find the best-fit model.

338 3. If the model did not describe the observed data well, the lines were re-fitted using just the
339 PCF. If that fit was also poor, then only the L-function was used.

340 4. 99 simulations of this model were generated to create simulation envelopes, and the fit
341 checked using the O-ring statistic (82).

342 5. In order to assess how well the model fit the observed data, the goodness-of-fit (p_d) was
343 calculated over the model range (86). A $p_d = 0$ indicates no model fit, and $p_d = 1$ indicates a
344 perfect model fit. Very small-scale segregations (of the order of specimen diameter) were not
345 included in the model fitting, since they likely represent the finite size of the specimens, and
346 a lack of specimen overlap.

347 6. If there were no excursions outside the simulation envelope and the p_d -value was high,
348 then a univariate homogeneous Thomas cluster model was interpreted as the best model.

349

350 For any univariate distributions exhibiting CSR, the size-classes of each taxon were
351 calculated, the univariate PCFs of the smallest size-classes and largest size-classes were
352 plotted, with 999 Monte Carlo simulations of a complete spatially random distribution and
353 segregation tests performed. The most objective way to resolve the number and range of size
354 classes in a population is by fitting height-frequency distribution data to various models,
355 followed by comparison of (logarithmically scaled) Bayesian information criterion (BIC)

356 values (86), which we performed in R using the package `MCLUST` (90). The number of
357 populations identified was then used to define the most appropriate size classes. A BIC
358 value difference of >10 corresponds to a “decisive” rejection of the hypothesis that two
359 models are the same, whereas values <6 indicate only weakly rejected similarity of the
360 models (90–94). Once defined, the PCFs for each size class were calculated.

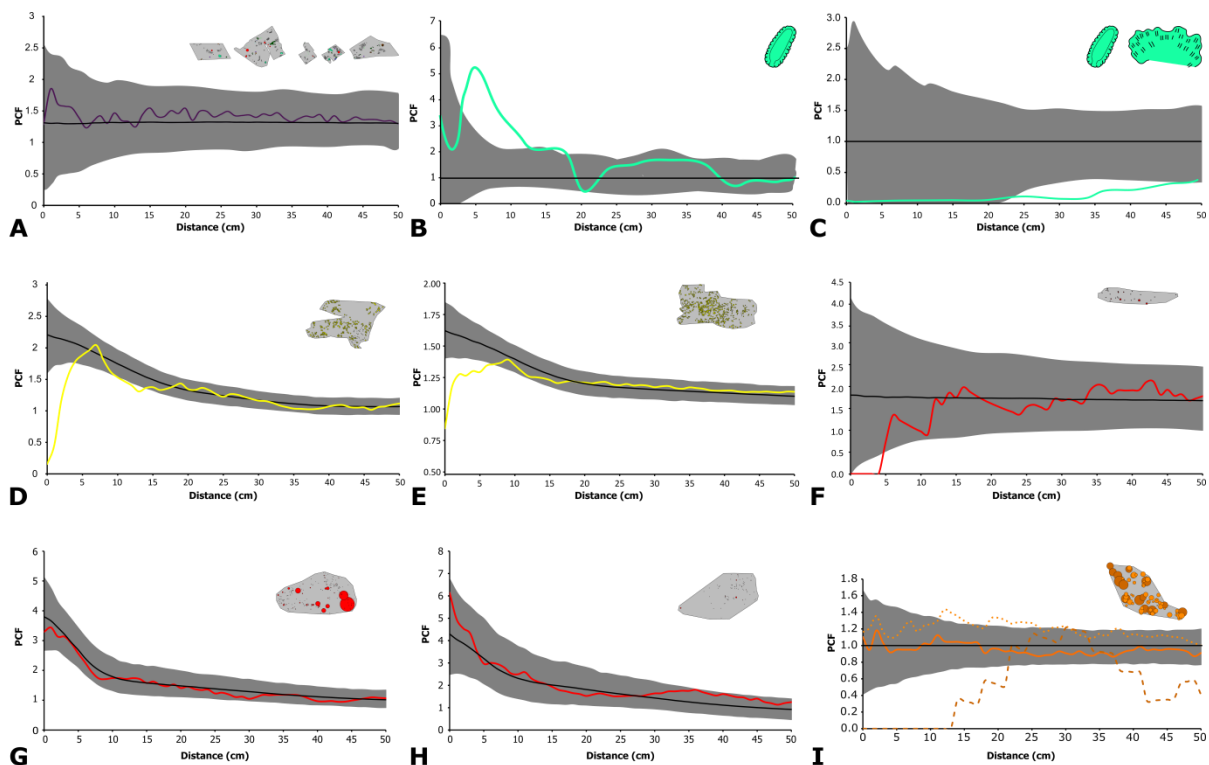
361

362 Bivariate analyses were performed on the KS surface (the only surface with multiple abundant
363 taxa/taxon groups) between *Kimberella* – *Orbisiana*, *Kimberella* – *Kimberichnus* and
364 *Orbisiana* – *Kimberichnus*. For each taxon pair, the bivariate PCF was calculated, and then
365 compared to CSR using Monte Carlo simulations and Diggle’s goodness-of-fit test.

366 **Results**

367 Across the seven palaeocommunities, *Dickinsonia* on the DS surface was the only taxon that
368 exhibited CSR. There were five univariate distributions (*Sessile Taxa* on KS, *Funisia* on FUN4
369 and FUN5, *Aspidella* on KH1 and KH2) exhibiting aggregated spatial distributions, two
370 univariate (*Aspidella* on WS and large *Dickinsonia* on DS) and one bivariate (*Kimberella* and
371 *Kimberichnus* on KS) segregated spatial distributions (Fig. 3, Table 2). The *Aspidella*
372 aggregations from KH1 and KH2 were best modelled by the same double Thomas cluster
373 process ($p_d^{kh1} = 0.883$, $p_d^{k21} = 0.932$, Fig. 3G, H; Table 2), which consisted of large clusters
374 of 20.96 cm diameter containing smaller clusters with a mean of six specimens within a cluster
375 of 7.34 cm in diameter (Fig. 3G and H, (95)). These results indicate that the non-random spatial
376 distributions were most likely due to two generations of reproduction cf. (47), and do not
377 represent a significant interaction or association with local habitat variations. This result is
378 consistent with previous work on older (~565 Ma) deep-water communities that also show a
379 strong non-environmentally influenced signal (23). In contrast, the *Aspidella* from the WS
380 surface show significant segregation and are best-modelled by a heterogeneous Poisson process

381 ($p_d^{ws} = 0.796$, Fig 3F, Table 2). This is consistent with small-scale intra-specific competition
 382 in a resource-limited environment (55). *Funisia* from FUN4 and FUN5 had aggregations that
 383 are best-modelled by heterogeneous Poisson processes ($p_d^{Fun4} = 0.9570$, $p_d^{Fun5} = 0.9080$, Fig.
 384 3 D, E; Table 2), which are interpreted to indicate significant habitat associations with the local
 385 environment.
 386



387 **Fig. 3. Pair correlation functions describing the spatial distributions of the seven studied**
 388 **palaeocommunities.** The coloured lines are the observed data and black lines represent best-
 389 fit models (either CSR or heterogeneous Poisson). The grey area is the simulation envelope
 390 for 999 Monte Carlo simulations. The x-axis is the inter-point distance between organisms in
 391 centimetres. On the y-axis, PCF = 1 indicates complete spatial randomness (CSR), < 1 indicates
 392 segregation, and > 1 indicates aggregation. A) The KS surfaces showing sessile specimens with
 393 the black-line showing the best-fit heterogeneous Poisson model. B) KS univariate *Kimberella*.
 394 C) KS bivariate *Kimberella* – *Kimberichnus* with the CSR model shown. D) FUN4, and E)
 395 FUN5 surfaces showing the *Funisia* distributions with the best-fit heterogeneous Poisson
 396

397 model. *Aspidella* from F) WS, G) KH1 and H) KH2 surfaces with their best-fit heterogeneous
 398 Poisson models. I) *Dickinsonia* from DS with the solid line showing the whole population,
 399 dotted line the juveniles and dashed line the adults with the CSR model shown.

400

SURFACE	TAXON	N	<i>P_d</i> VALUES PCF				
			CSR	HP	TC	DTC	ITC
WS	<i>Aspidella</i>	40	0.019	0.796	0.504	0.2759	0.425
KH1	<i>Aspidella</i>	204	0.001	0.001	0.648	0.883	0.313
KH2	<i>Aspidella</i>	81	0.001	0.001	0.576	0.932	0.001
FUN4	<i>Funisia</i>	290	0.001	0.9570	0.6340	NA	0.245
FUN5	<i>Funisia</i>	482	0.001	0.9080	0.1320	NA	0.218
DS	<i>Dickinsonia</i>	62	0.857	0.022	0.025	NA	0.019
	<i>Dickinsonia</i> Small	48	0.128	0.978	0.143	NA	0.158
	<i>Dickinsonia</i> Large	14	0.388	0.446	0.409	NA	0.434
KS	All	107	0.858	0.381	0.328	NA	0.380
	<i>All sessile</i>	44	0.033	0.956	0.770	NA	0.761
	<i>Kimberella</i>	18	0.001	0.837	0.491	NA	0.103
	<i>Orbisiana</i>	16	0.325	0.332	0.326	NA	0.288
	<i>Kimberichnus</i>	6	0.566	NA	NA	NA	NA
	Bivariate <i>Kimberella</i> – <i>Kimberichnus</i>	24	0.028	NA	NA	NA	NA

401

402 **Table 2. Goodness-of-fit tests for spatial analyses.** For the inhomogeneous point processes
 403 (HP and ITC), the moving window radius is 0.5 m, using the same taxon density as the taxon
 404 being modelled. $p_d = 1$ corresponds to a perfect fit of the model to the data, while $p_d = 0$
 405 corresponds to no fit. Where observed data did not fall outside CSR Monte-Carlo simulation
 406 envelopes, no further analyses were performed, which is indicated by NA. CSR: Complete
 407 spatial randomness indicates, HP: Heterogeneous Poisson model, TC: Thomas cluster model,
 408 DTC: double Thomas Cluster, and ITC: inhomogeneous Thomas cluster model. N is the
 409 number of specimens mapped. Note that for the mobile taxa *Dickinsonia* and *Kimberella*, and
 410 presumed trace fossils formed by mobile taxa (*Kimberichnus*), the observed spatial pattern will
 411 also be defined by their behaviour, and so the inference of process from pattern is not as
 412 straightforward (see discussion in the main text). The p_d -value of the best-fit model is given
 413 in bold.

414

415 The KS community is notably different in species composition from deep-water communities
416 because it contains mobile organisms such as *Kimberella* and *Yorgia* (96–99) as well as
417 putative trace fossils such as *Radulichus* (thought to be produced by the grazing activity of
418 *Kimberella* specimens) (100). We found that the KS community exhibits CSR, which suggests
419 that any taxon-specific univariate distributions are likely to be biological/ecological in origin,
420 rather than resulting from a taphonomic bias ($p_d^{KS_{All}} = 0.858$, Table 2, (23)). In contrast, when
421 all the sessile taxa were grouped together they exhibited a significant aggregation (Table 2),
422 which was best-modelled by a heterogeneous Poisson process ($p_d^{KS_{Sessile}} = 0.956$, Table 2).
423 *Kimberella* exhibits a significant aggregation under spatial scales of 20 cm ($p_d^{KS_{Kimberella}}$
424 $= 0.001$ for CSR model, Fig. 3A), with Thomas cluster and heterogeneous Poisson models
425 fitting the data well, suggesting that behaviour factors may also influence *Kimberella* spatial
426 patterns. The *Kimberichnus* PCF spatial distribution has a CSR distribution (Fig. 3B, $p_d^{KS_{Rad}}$
427 $= 0.566$, Table 2). Furthermore, the bivariate analyses between *Kimberella* and *Kimberichnus*
428 show a significant segregation ($p_d^{KS_{KimRad}} = 0.028$, Fig 3C), which could reflect the *Kimberella*
429 organisms avoiding patches of the surface that had already been grazed.

430

431 The *Dickinsonia* population from DS exhibited a CSR PCF distribution (Fig 3I, $p_d = 0.857$).
432 Analysis of the population of *Dickinsonia* from DS showed two cohorts in the size-distribution
433 (95). The two cohorts exhibited different PCF spatial behavior, with the small specimens
434 aggregating with a best-fit heterogeneous Poisson model (Fig 3I, $p_d^{small} = 0.978$) and the large
435 specimens exhibiting segregation (Fig. 3I).

436

437 **Interpreting the spatial distributions of mobile organisms**

438 For mobile organisms, inferring the underlying process behind the observed spatial
439 distributions is imprecise, since their spatial patterns also incorporate contributions from their

440 behavior. Modern animals move primarily to find resources, mates, microhabitats and/or
441 escape predators or detrimental environmental conditions. There is no evidence for predators
442 until the terminal Ediacaran (101), and although we cannot definitely rule out reproductive
443 aggregations, they are also considered unlikely because the largest size-class in the studied
444 *Dickinsonia* population exhibits univariate segregation, so at time-of-burial, the organisms
445 were not aggregating as might be expected in a mating event. Furthermore, the majority of
446 extant marine benthic organisms use broadcast spawning to reproduce sexually (102), so do
447 not require the two mating organisms to be within the spatial scale (< 40 cm) found on the DS
448 surface. We cannot determine whether the large *Dickinsonia* are reacting to the mortality event
449 which killed and preserved them, however, this would not explain the complex interplay
450 between aggregation and segregated behaviors. Therefore, for this *Dickinsonia* population, the
451 search for resources and/or microhabitats is considered most plausible explanation, particularly
452 since this hypothesis is further supported by their spatial patterns. Aggregated – segregated
453 PCF patterns such as those seen in our *Dickinsonia* population are common in extant sessile
454 organisms where juveniles are initially aggregated on preferred habitats but then begin to
455 compete with each other as they require greater resources, leading to thinning or segregation
456 amongst adult populations (55). While it is not possible to confirm the underlying mechanism
457 for the distribution of the studied *Dickinsonia* population, we consider it most likely to be
458 motivated by associations with preferential habitat for food and/or resources. Further analyses
459 of other *Dickinsonia* surfaces would enable more robust conclusions to be reached.

460

461 **Time averaging**

462 The preservation of time-averaged communities has the potential to bias our analyses (see
463 (21,25). In Avalonian communities, taphomorphs interpreted to record the decaying remains
464 of organisms are identified by their poor preservational fidelity, irregular morphologies, and

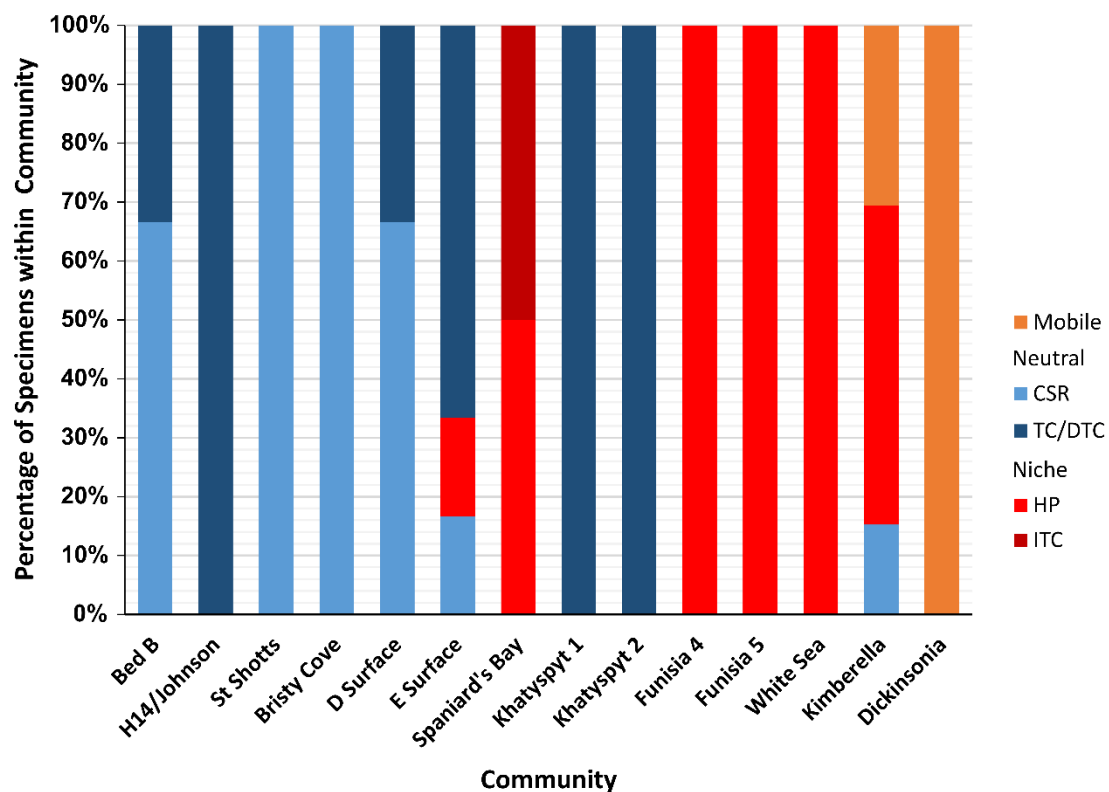
465 often high topographic relief (103). This interpretation is consistent with data suggesting that
466 the spatial interactions of some taphomorph populations mirror those of other taxa they are
467 considered to be derived from (21). Taphomorphs are considered unlikely to have imparted a
468 significant signal on these studied surfaces, since we did not observe ivesheadiomorph-type
469 forms, and there is a consistent level of preservational detail amongst fossil communities
470
471 *Funisia* communities tend to have very similar diameters for the holdfasts, which suggests
472 single colonization events (104). Different reproductive events can be distinguished by
473 population analyses of size-distributions (105), with each reproductive event identified through
474 statistically significant cohorts within the size-distribution (90). Surfaces FUN4 and FUN5
475 both exhibit populations with two cohorts (SI Figure 1), most likely indicating two
476 reproductive/colonization events. The best-fit models for each of these surfaces are
477 heterogeneous Poisson models (Fig. 3, Table 2), with very high goodness-of-fit values ($p_d >$
478 0.90) reflecting a single model for each surface. Therefore, cohorts of *Funisia* specimens on
479 each of the studied surfaces were affected by the same underlying environmental heterogeneity,
480 so most likely were contemporaneous.

481

482 **Discussion**

483 The univariate and bivariate analyses of five out of seven of the studied palaeocommunities
484 provide compelling evidence that their local environment had a significant influence on their
485 communities (Fig. 3, Table 2). In modern settings, habitat associations form when a patchy
486 resource provides heterogeneously distributed preferential conditions for the establishment and
487 growth of sessile taxa, and/or feeding ‘hotspots’ for the mobile taxa (47,54,83). The presence
488 of inferred habitat interactions within our palaeocommunities showed a significant correlation
489 with the environmental setting (Kruskal-Wallis Test, $p = 0.049$), with all five

490 palaeocommunities with strong habitat interactions derived from shallow-water settings. The
491 two communities that were seemingly not strongly influenced by their local habitat are from
492 deep-water facies (Table 2). These results are consistent with previous work, which found
493 that for seven independent deep-marine (slope and basin) Ediacaran palaeocommunities from
494 Newfoundland and Charnwood Forest, only one was dominated by associations of taxa with
495 local habitat heterogeneities (21–23) (Kruskal-Wallis Test of all data, $p = 0.021$; Fig. 4).
496



497
498 **Fig. 4 Proportion of best-fit univariate models by surface, adapted from (23).** The
499 percentage of specimens within the community with univariate spatial distributions that are
500 best described by CSR, HP, TC (or DTC) and ITC models. CSR and TC are considered random
501 or dispersal (neutral) models and are shown in blue. HP and ITC are local environmentally
502 driven (niche) models, shown in red. Mobile taxa are shown in orange, and inferred to be
503 environmentally-driven. Data and plot for surfaces Bed B to Spaniard's Bay from ref. (23).

504

505 Untangling environmental from evolutionary trends in the Ediacaran has been hampered by a
506 limited overlap between temporal periods and environmental settings (1,17). The
507 palaeocommunities in this study derive from successions within a variety of lithologies (tuff,
508 coarse sandstone, mixed siltstone, limestone) as well as palaeogeographic positions
509 (17,62,63,69,104,106,107). We find no significant direct correlations between these factors and
510 the relative importance of habitat heterogeneities on the studied surfaces ($p \gg 0.1$; Fig. 3,
511 Table 2). The palaeocommunities that are not influenced by local habitat heterogeneities (KH1
512 and KH2) are hosted within carbonate successions (107), making them distinct from the
513 siliciclastically-hosted palaeocommunities on the KS, WS, FUN4, FUN5 and DS surfaces, or
514 in previous (21–23) work. However, the Khatyspyt surfaces behave ecologically in the same
515 way to Avalonian palaeocommunities derived from similar depths, but different lithological
516 successions (21–23), suggesting that lithology alone is not causing the KH1 and KH2 surfaces
517 differing results. Therefore, two possible factors remain that may explain the differences in
518 community dynamics found here. The differences could reflect evolutionary trends, and it is
519 true that the oldest studied palaeocommunities show limited habitat influence (21–23), when
520 compared to the younger palaeocommunities documented in this study (Fig. 4). Unfortunately,
521 the lack of fine-scale dating across these communities and older Avalonian ones precludes
522 detailed fine-scale regression to assess whether either the Khatyspyt palaeocommunities are an
523 outlier to this apparent trend, or this trend merely reflects the biases of the available data.
524 Alternatively, the differences could be due to the environmental setting. We have shown that
525 Ediacaran environmental setting has a significant influence on community dynamics ($p =$
526 0.021), with shallow water palaeocommunities significantly influenced by habitat
527 heterogeneities, in contrast to the deep water palaeocommunities (Fig 3, Table 2; (21–23)).

528

529 While SPPA have only been applied to a small proportion of the known in-situ Ediacaran
530 palaeocommunities (17 studied surfaces (21–23,23,60,108)), there is a notable correspondence
531 between the importance of habitat heterogeneities to community ecology and assemblage
532 diversity. In this study, the palaeocommunities exhibiting significant influence from local
533 habitat heterogeneities are those that belong to the diverse White Sea assemblage, which is in
534 contrast to the previous work on Avalonian palaeocommunities (21–23), which are not
535 significantly influenced by such heterogeneities. The relationship between environmental
536 spatial heterogeneities and species richness is well established, with habitat variations enabling
537 species co-existence through the creation of different niches (109). This relationship extends
538 to modern deep-sea benthic communities, where these heterogeneities have been shown to
539 provide a mechanism for diversification on large scales, such as between canyons, trenches,
540 seamounts (110,111), on the centimetre to metre scale (112), and through microhabitats (45).

541

542 Tentatively, we propose that the ecological differentiation observed between Ediacaran
543 shallow and deep-water communities may evidence the late Ediacaran development of a chain
544 of evolutionary diversification. This chain started in shallow water communities, with the
545 creation of habitat patchiness by mobile Ediacaran organisms, which then led to a feedback of
546 increasing diversification that ultimately expanded into the deep-sea. This hypothesized
547 feedback could have promoted diversification throughout the Ediacaran by increasing
548 heterogeneity as follows:

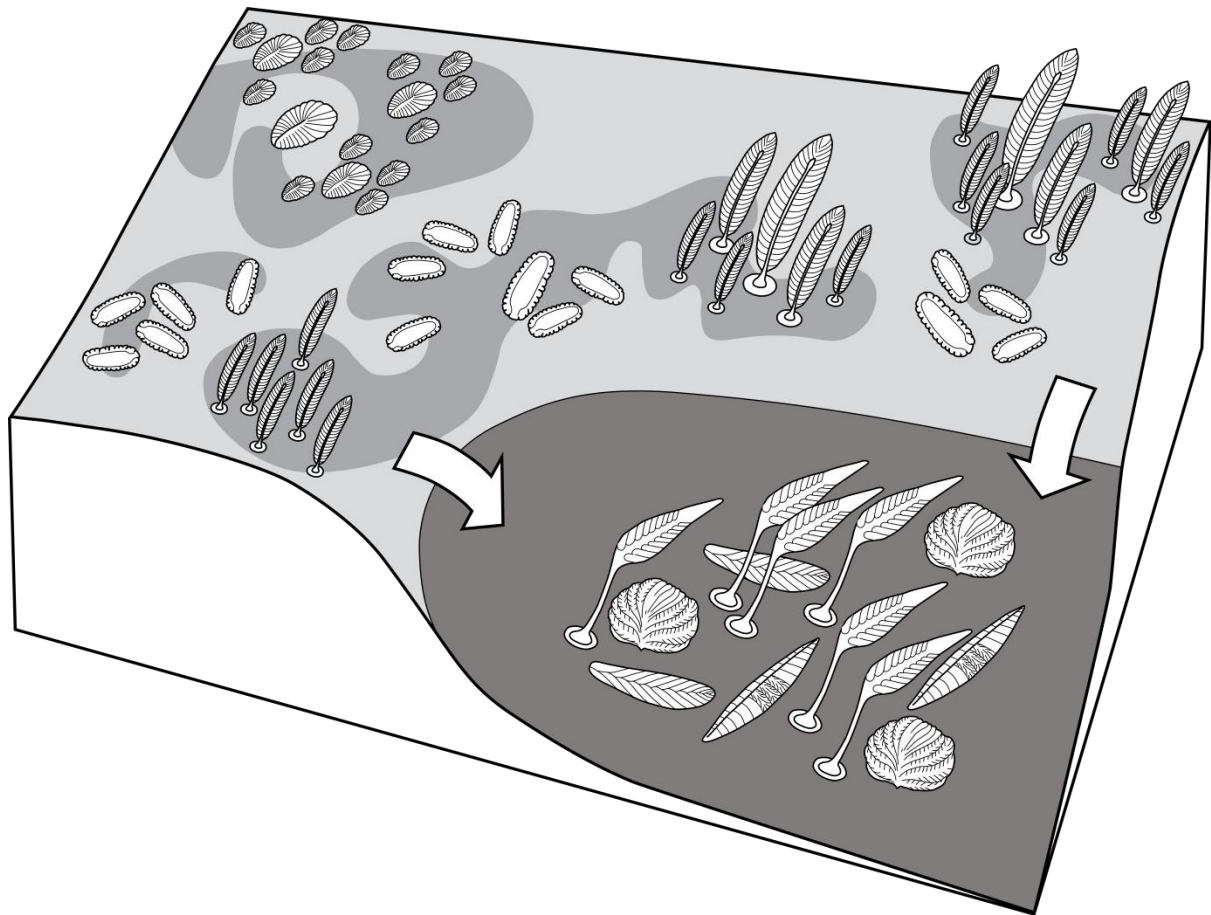
549

550 First, metazoan mat grazing creates spatial heterogeneity in microbial substrates through the
551 formation of depleted and non-depleted patches (113). Our data suggest that once created,
552 organisms such as *Kimberella* may have avoided pre-grazed patches, with this selective grazing
553 accelerating further creation of mat heterogeneity (Fig 3C). Secondly, the grazing-induced

554 creation of different-sized detrital particles in the form of differential-sized fecal pellets and
555 fragments of non-consumed food within the water-column (114), would have created new food
556 sources and therefore potential new niches. Thirdly, this shallow-water differentiated
557 particulate organic carbon (POC) and matter (POM) could have eventually filtered through to
558 deep-sea communities, promoting deep-sea heterogeneity. In the modern ocean, the main
559 source of deep-sea habitat heterogeneity is small-scale variation due to differentiated particle
560 influx (114), with the majority of the particulate organic carbon (POC) coming from
561 phytodetritus, which is transported from shallow waters to deep waters by ocean currents, tides
562 and upwelling (114,116). In the modern ocean, the diurnal vertical migration of
563 mesozooplankton and macrofauna contributes up to 50% of POC to the deep-sea via fecal
564 pellets (116–118). A planktonic/larval stage for Ediacaran organisms has been predicted on
565 the basis of their likely waterborne dispersal mechanisms (25,105), but there is presently no
566 direct evidence of non-larval, planktotrophic zooplankton until the onset of the Cambrian
567 (119). In the absence of planktotrophic zooplankton and macrofauna, the Ediacaran POC flux
568 may have been either larger, due to lack of consumption of phytoplankton in the shallow water,
569 or smaller, due to a lack of mixing by diurnal vertical migration of the plankton (6), and this
570 cannot yet be determined. However, the other ~50% of POC flux in the modern oceans is
571 transported from shallow to deep-water via oceanic currents and upwelling (114,116), which
572 should still have operated in the Ediacaran. However, prior to grazers and detritivores, this
573 POC/POM flux would have been relatively homogenous phytodetritus. The evolution of
574 grazers would have led to a shift towards size differentiated POC/POM, potentially increasing
575 the heterogeneity of the deep-sea landscape (114), and providing a mechanism for deep-marine
576 diversification.
577

578 Budd and Jensen (12) introduced the Savannah hypothesis to explain early animal
579 diversification, whereby Ediacaran diversification was driven by small-scale variations in local
580 habitat. They argued that it was the drive to find these heterogeneous distributed resources that
581 led to novel evolutionary innovations such as mobility. Our results demonstrate that at least
582 some of these early animal communities that contain mobile organisms were influenced by
583 such habitat variations, and we describe a mechanism that links early animal diversification
584 and benthic habitat patchiness prior to the evolution of predators and wide-spread pelagic
585 organisms. We show that taxa such as *Kimberella* had a segregated distribution with trace
586 fossils considered to be their grazing traces (98), suggesting that they may have been capable
587 of avoiding non-preferred areas, possibly already consumed patches, revealing adaptation of
588 behavior when interacting with these patches. This adaptation theoretically has the capacity to
589 drive further diversification, initially dependent on the environmental-setting, starting in the
590 shallow water, and then, over time, moving into deeper water, but currently available global
591 fossil assemblages limit the testing of this prediction. If this hypothesis is correct, we would
592 expect deep-water assemblages to diversify during the terminal Ediacaran and into the
593 Cambrian. Our results therefore provide tentative support for the Savannah hypothesis,
594 suggesting that this late Ediacaran taxonomic diversification was a benthic event, which
595 facilitated a chain of diversification by promoting marine habitat heterogeneities.

596



597

598 **Fig. 5. Schematic diagram showing variation of heterogeneities within different**
599 **environmental settings.** Shallow water communities are significantly influenced by habitat
600 heterogeneities. Grazing within these shallow waters further increases substrate heterogeneity,
601 potentially increasing diversification. Furthermore, this grazing increases deep-water
602 heterogeneity through the creation of different sized particulate organic matter due to the influx
603 of particulate matter from the shallows.

604

605 **Conclusions**

606 We present evidence to suggest that the influence of local habitat on Ediacaran organisms is
607 significantly correlated with broad-scale environmental setting. The relationship of Ediacaran
608 communities to habitat-dependent interactions is correlated with Ediacaran assemblage
609 diversity, with communities from the more diverse White Sea assemblage showing significant

610 habitat associations and interactions in contrast to relatively habitat insensitive deep-sea
611 Avalonian assemblages. We suggest that the presence of shallow-water grazers could have
612 created further habitat heterogeneity in shallow-water and ultimately deep-water, via the
613 heterogenization of the shallow-water substrate and via the introduction of variable size
614 particulate matter to the deep-sea. These results demonstrate the utility of these approaches for
615 investigating the early diversification of metazoans. We have shown the importance of local
616 environmental patchiness to the diversification of early animals, and our results are consistent
617 with the hypothesis that the early diversification of metazoans was a benthic event, driven by
618 responses to habitat patchiness.

619

620 **Acknowledgements**

621 We thank K. Nagovitsin and O. Zharasbayev (IPGG SB RAS) for help with mapping surfaces
622 KH1 and KH2, and J. Gehling and M. Binnie of the South Australia Museum for assisting with
623 access to Australian material.

624

625 **Funding**

626 This work has been supported by the Natural Environment Research Council [grant numbers
627 NE/P002412/1 and Independent Research Fellowship NE/S014756/1 EGM, and Independent
628 Research Fellowship NE/L011409/2 to AGL], a Gibbs Travelling Fellowship (2016-2017)
629 from Newnham College, Cambridge, and a Henslow Research Fellowship from Cambridge
630 Philosophical Society to EGM (2016-2019). Field research in the White Sea Region, Arctic
631 Siberia and Central Urals has been supported by the Russian Science Foundation [grant number
632 17-17-01241 to DG]. SX acknowledges funding from the NASA Exobiology and Evolutionary
633 Biology Program [80NSSC18K1086]. Large image processing and interpretation of

634 photomontages of the *Dickinsonia* Surface was supported by the Russian Foundation for Basic
635 Research [grant number 19-05-00828 to AVK].

636

637 **References**

638 1. Wood R, Liu AG, Bowyer F, Wilby PR, Dunn FS, Kenchington CG, et al. Integrated
639 records of environmental change and evolution challenge the Cambrian Explosion. *Nat*
640 *Ecol Evol.* 2019;3(4):528–38.

641 2. Xiao S, Laflamme M. On the eve of animal radiation: phylogeny, ecology and evolution
642 of the Ediacara biota. *Trends in Ecology and Evolution.* 2009;24(1):31–40.

643 3. Erwin DH, Laflamme M, Tweedt SM, Sperling EA, Pisani D, Peterson KJ. The Cambrian
644 Conundrum: Early Divergence and Later Ecological Success in the Early History of
645 Animals. *Science.* 2011 Nov 25;334(6059):1091–7.

646 4. Lenton TM, Boyle RA, Poulton SW, Shields-Zhou GA, Butterfield NJ. Co-evolution of
647 eukaryotes and ocean oxygenation in the Neoproterozoic era. *Nature Geoscience.*
648 2014;7(4):257–65.

649 5. Butterfield NJ. Macroevolutionary turnover through the Ediacaran transition: ecological
650 and biogeochemical implications. Geological Society, London, Special Publications.
651 2009;326(1):55–66.

652 6. Butterfield NJ. Oxygen, animals and aquatic bioturbation: An updated account.
653 *Geobiology.* 2018;16(1):3–16.

654 7. Sperling EA, Frieder CA, Raman AV, Girguis PR, Levin LA, Knoll AH. Oxygen, ecology,
655 and the Cambrian radiation of animals. *PNAS.* 2013 Aug 13;110(33):13446–51.

656 8. Lenton TM, Daines SJ. The effects of marine eukaryote evolution on phosphorus, carbon
657 and oxygen cycling across the Proterozoic–Phanerozoic transition. *Emerging Topics in*
658 *Life Sciences.* 2018;2(2):267–78.

- 659 9. Wood R, Erwin DH. Innovation not recovery: dynamic redox promotes metazoan
660 radiations. *Biological Reviews*. 2018;93(2):863–73.
- 661 10. Butterfield NJ. Animals and the invention of the Phanerozoic Earth system. *Trends in*
662 *Ecology & Evolution*. 2011 Feb 1;26(2):81–7.
- 663 11. Mángano MG, Buatois LA. Decoupling of body-plan diversification and ecological
664 structuring during the Ediacaran–Cambrian transition: evolutionary and geobiological
665 feedbacks. *Proceedings of the Royal Society B: Biological Sciences*. 2014 Apr
666 7;281(1780):20140038.
- 667 12. Budd GE, Jensen S. The origin of the animals and a ‘Savannah’ hypothesis for early
668 bilaterian evolution. *Biological Reviews*. 2017;92(1):446–73.
- 669 13. Muscente AD, Boag TH, Bykova N, Schiffbauer JD. Environmental disturbance, resource
670 availability, and biologic turnover at the dawn of animal life. *Earth-Science Reviews*. 2018
671 Feb 1;177:248–64.
- 672 14. McPeck MA. The Ecological Dynamics of Natural Selection: Traits and the Coevolution
673 of Community Structure. *The American Naturalist*. 2017 May 1;189(5):E91–117.
- 674 15. Waggoner B. The Ediacaran Biotas in Space and Time. *Integr Comp Biol*. 2003 Feb
675 1;43(1):104–13.
- 676 16. Grazhdankin D. Patterns of distribution in the Ediacaran biotas: facies versus biogeography
677 and evolution. *Paleobiology*. 2004 Mar 1;30(2):203–21.
- 678 17. Boag TH, Darroch SAF, Laflamme M. Ediacaran distributions in space and time: testing
679 assemblage concepts of earliest macroscopic body fossils. *Paleobiology*. 2016;42(4):574–
680 94.
- 681 18. Wood DA, Dalrymple RW, Narbonne GM, Gehling JG, Clapham ME. Paleoenvironmental
682 analysis of the late Neoproterozoic Mistaken Point and Trepassy formations, southeastern
683 Newfoundland. *Canadian Journal of Earth Sciences*. 2003 Oct 1;40(10):1375–91.

- 684 19. Gehling JG, Droser ML. How well do fossil assemblages of the Ediacara Biota tell time?
685 Geology. 2013 Apr 1;41(4):447–50.
- 686 20. Clapham ME, Narbonne GM, Gehling JG. Paleocology of the oldest known animal
687 communities: Ediacaran assemblages at Mistaken Point, Newfoundland. Paleobiology.
688 2003;29(4):527–44.
- 689 21. Mitchell EG, Butterfield NJ. Spatial analyses of Ediacaran communities at Mistaken Point.
690 Paleobiology. 2018 Feb 1;44(1):40–57.
- 691 22. Mitchell EG, Kenchington CG. The utility of height for the Ediacaran organisms of
692 Mistaken Point. Nat Ecol Evol. 2018 Aug;2(8):1218–22.
- 693 23. Mitchell EG, Harris S, Kenchington CG, Vixseboxse P, Roberts L, Clark C, et al. The
694 importance of neutral over niche processes in structuring Ediacaran early animal
695 communities. Ecology Letters. 2019;22(12):2028–38.
- 696 24. Coutts FJ, Gehling JG, García-Bellido DC. How diverse were early animal communities?
697 An example from Ediacara Conservation Park, Flinders Ranges, South Australia.
698 Alcheringa: An Australasian Journal of Palaeontology. 2016 Oct 24;40(4):407–21.
- 699 25. Mitchell EG, Kenchington CG, Liu AG, Matthews JJ, Butterfield NJ. Reconstructing the
700 reproductive mode of an Ediacaran macro-organism. Nature. 2015 Aug;524(7565):343–6.
- 701 26. Wilby PR, Carney JN, Howe MPA. A rich Ediacaran assemblage from eastern Avalonia:
702 Evidence of early widespread diversity in the deep ocean. Geology. 2011;39(7):655–8.
- 703 27. Narbonne GM. THE EDIACARA BIOTA: Neoproterozoic Origin of Animals and Their
704 Ecosystems. Annual Review of Earth and Planetary Sciences. 2005;33(1):421–42.
- 705 28. Pu JP, Bowring SA, Ramezani J, Myrow P, Raub TD, Landing E, et al. Dodging snowballs:
706 Geochronology of the Gaskiers glaciation and the first appearance of the Ediacaran biota.
707 Geology. 2016;44(11):955–8.

- 708 29. Noble SR, Condon DJ, Carney JN, Wilby PR, Pharaoh TC, Ford TD. U-Pb geochronology
709 and global context of the Charnian Supergroup, UK: Constraints on the age of key
710 Ediacaran fossil assemblages. *GSA Bulletin*. 2015 Jan 1;127(1–2):250–65.
- 711 30. Bush AM, Bambach RK, Erwin DH. Ecospace Utilization During the Ediacaran Radiation
712 and the Cambrian Eco-explosion. *Quantifying the Evolution of Early Life*. 2011;111–33.
- 713 31. Shen B, Dong L, Xiao S, Kowalewski M. The Avalon Explosion: Evolution of Ediacara
714 Morphospace. *Science*. 2008 Jan 4;319(5859):81–4.
- 715 32. Liu AG, McIlroy D, Brasier MD. First evidence for locomotion in the Ediacara biota from
716 the 565 Ma Mistaken Point Formation, Newfoundland. *Geology*. 2010 Feb 1;38(2):123–6.
- 717 33. Gage JD, Tyler PA. Re-appraisal of age composition, growth and survivorship of the deep-
718 sea brittle star *Ophiura ljungmani* from size
719 structure in a sample time series from the Rockall Trough. *Mar Biol*. 1981 Sep
720 1;64(2):163–72.
- 721 34. Tecchio S, Ramírez-Llodra E, Sardà F, Company JB. Biodiversity of deep-sea demersal
722 megafauna in western and central Mediterranean basins. *Scientia Marina*. 2011;75(2):341–
723 50.
- 724 35. Seilacher A, Grazhdankin D, Legouta A. Ediacaran biota: The dawn of animal life in the
725 shadow of giant protists. *Paleontological Research*. 2003;7(1):43–54.
- 726 36. Droser ML, Gehling JG. The advent of animals: The view from the Ediacaran. *PNAS*. 2015
727 Apr 21;112(16):4865–70.
- 728 37. Duda J-P, Blumenberg M, Thiel V, Simon K, Zhu M, Reitner J. Geobiology of a
729 palaeoecosystem with Ediacara-type fossils: The Shibantan Member (Dengying
730 Formation, South China). *Precambrian Research*. 2014 Dec 1;255:48–62.
- 731 38. Chen Z, Chen X, Zhou C, Yuan X, Xiao S. Late Ediacaran trackways produced by
732 bilaterian animals with paired appendages. *Science Advances*. 2018 Jun 1;4(6):eaao6691.

- 733 39. Sperling EA, Vinther J. A placozoan affinity for Dickinsonia and the evolution of late
734 Proterozoic metazoan feeding modes. *Evolution & Development*. 2010;12(2):201–9.
- 735 40. Gehling JG, Droser ML. Ediacaran scavenging as a prelude to predation. *Emerging Topics*
736 *in Life Sciences*. 2018;2(2):213–22.
- 737 41. Seilacher A, Buatois LA, Gabriela Mángano M. Trace fossils in the Ediacaran–Cambrian
738 transition: Behavioral diversification, ecological turnover and environmental shift.
739 *Palaeogeography, Palaeoclimatology, Palaeoecology*. 2005 Nov 10;227(4):323–56.
- 740 42. Droser ML, Gehling JG, Tarhan LG, Evans SD, Hall CMS, Hughes IV, et al. Piecing
741 together the puzzle of the Ediacara Biota: Excavation and reconstruction at the Ediacara
742 National Heritage site Nilpena (South Australia). *Palaeogeography, Palaeoclimatology,*
743 *Palaeoecology*. 2019 Jan 1;513:132–45.
- 744 43. Reid LM, García-Bellido DC, Gehling JG. An Ediacaran opportunist? Characteristics of a
745 juvenile Dickinsonia costata population from Crisp Gorge, South Australia Reid et al. --
746 Population analysis of Dickinsonia costata from South Australia *Journal of Paleontology*.
747 *Journal of Paleontology*. 2018;92(3):313–22.
- 748 44. Finnegan S, Gehling JG, Droser ML. Unusually variable paleocommunity composition in
749 the oldest metazoan fossil assemblages. *Paleobiology*. 2019 May;45(2):235–45.
- 750 45. Kukert H, Smith CR. Disturbance, colonization and succession in a deep-sea sediment
751 community: artificial-mound experiments. *Deep Sea Research Part A Oceanographic*
752 *Research Papers*. 1992 Jul 1;39(7):1349–71.
- 753 46. Liu AG, Kenchington CG, Mitchell EG. Remarkable insights into the paleoecology of the
754 Avalonian Ediacaran macrobiota. *Gondwana Research*. 2015 Jun 1;27(4):1355–80.
- 755 47. Illian DJ, Penttinen PA, Stoyan DH, Stoyan DD. *Statistical Analysis and Modelling of*
756 *Spatial Point Patterns*. John Wiley & Sons; 2008. 557 p.

- 757 48. Wiegand T, Gunatilleke S, Gunatilleke N, Okuda T. Analyzing the Spatial Structure of a
758 Sri Lankan Tree Species with Multiple Scales of Clustering. *Ecology*. 2007;88(12):3088–
759 102.
- 760 49. Seidler TG, Plotkin JB. Seed Dispersal and Spatial Pattern in Tropical Trees. *PLOS*
761 *Biology*. 2006 Oct 17;4(11):e344.
- 762 50. Getzin S, Dean C, He F, Trofymow JA, Wiegand K, Wiegand T. Spatial patterns and
763 competition of tree species in a Douglas-fir chronosequence on Vancouver Island.
764 *Ecography*. 2006;29(5):671–82.
- 765 51. Lingua E, Cherubini P, Motta R, Nola P. Spatial structure along an altitudinal gradient in
766 the Italian central Alps suggests competition and facilitation among coniferous species.
767 *Journal of Vegetation Science*. 2008;19(3):425–36.
- 768 52. Getzin S, Dean C, He F, Trofymow JA, Wiegand K, Wiegand T. Heterogeneity influences
769 spatial patterns and demographics in forest stands. *Journal of Ecology*. 2008;96(4):807–
770 20.
- 771 53. Harms KE, Wright SJ, Calderón O, Hernández A, Herre EA. Pervasive density-dependent
772 recruitment enhances seedling diversity in a tropical forest. *Nature*. 2000
773 Mar;404(6777):493–5.
- 774 54. Lin Y-C, Chang L-W, Yang K-C, Wang H-H, Sun I-F. Point patterns of tree distribution
775 determined by habitat heterogeneity and dispersal limitation. *Oecologia*. 2011 Jan
776 1;165(1):175–84.
- 777 55. Kenkel NC. Pattern of Self-Thinning in Jack Pine: Testing the Random Mortality
778 Hypothesis. *Ecology*. 1988;69(4):1017–24.
- 779 56. Diggle P, Zheng P, Durr P. Nonparametric estimation of spatial segregation in a
780 multivariate point process: bovine tuberculosis in Cornwall, UK. *Journal of the Royal*
781 *Statistical Society: Series C (Applied Statistics)*. 2005;54(3):645–58.

- 782 57. Law R, Illian J, Burslem DFRP, Gratzner G, Gunatilleke CVS, Gunatilleke I a. UN.
783 Ecological information from spatial patterns of plants: insights from point process theory.
784 Journal of Ecology. 2009;97(4):616–28.
- 785 58. Comita L, Condit R, Hubbell SP. Developmental changes in habitat associations of tropical
786 trees. Journal of Ecology. 2007;95:482–92.
- 787 59. Wiegand T, Moloney KA, Moloney KA. Handbook of Spatial Point-Pattern Analysis in
788 Ecology. 1st ed. Chapman and Hall/CRC; 2013.
- 789 60. Mitchell EG, Kenchington CG, Harris S, Wilby PR. Revealing rangeomorph species
790 characters using spatial analyses. Canadian Journal of Earth Sciences. 2018 Nov
791 1;55(11):1262–70.
- 792 61. Grazhdankin D. The Ediacaran genus *Inaria*: a taphonomical morphodynamic analysis.
793 Neues Jahrbuch für Geologie und Paläontologie - Abhandlungen. 2000 Apr 18;1–34.
- 794 62. Grazhdankin DV. Structure and Depositional Environment of the Vendian Complex in the
795 Southeastern White Sea Area. Stratigraphy and Geological Correlation. 2003;11(4):313–
796 31.
- 797 63. Grazhdankin DV, Maslov AV, Krupenin MT. Structure and depositional history of the
798 Vendian Sylvitsa Group in the western flank of the Central Urals. Stratigr Geol Correl.
799 2009 Oct 9;17(5):476.
- 800 64. Schmitz M, editor. In: The Geologic Time Scale 2012. Elsevier; 2012. p. 1045–1082.
- 801 65. Martin MW, Grazhdankin DV, Bowring SA, Evans D a. D, Fedonkin MA, Kirschvink JL.
802 Age of Neoproterozoic Bilatarians and Trace Fossils, White Sea, Russia: Implications
803 for Metazoan Evolution. Science. 2000;288(5467):841–5.
- 804 66. Droser ML, Gehling JG, Dzaugis ME, Kennedy MJ, Rice D, Allen MF. A New Ediacaran
805 Fossil with a Novel Sediment Displacive Life Habit A New Ediacaran fossil with a Novel
806 Life Habit. Journal of Paleontology. 2014 Jan 1;88(1):145–51.

- 807 67. Tarhan LG, Droser ML, Gehling JG, Dzaugis MP. Taphonomy and morphology of the
808 Ediacara form genus *Aspidella*. *Precambrian Research*. 2015 Feb 1;257:124–36.
- 809 68. Reid LM, Payne JL, García-Bellido DC, Jago JB. The Ediacara Member, South Australia:
810 lithofacies and palaeoenvironments of the Ediacara biota. *Gondwana Research* [Internet].
811 2019 Nov 7 [cited 2019 Nov 13]; Available from:
812 <http://www.sciencedirect.com/science/article/pii/S1342937X19302862>
- 813 69. Grazhdankin DV, Maslov AV, Krupenin Mt, Mustill Tmr. The Ediacaran White Sea biota
814 in the Central Urals. *Doklady Earth Sciences*. 2005;401A(3):382–5.
- 815 70. Bobkov NI, Kolesnikov AV, Maslov AV, Grazhdankin D. The occurrence of *Dickinsonia*
816 in non-marine facies. *Estudios geológicos*. 75(2):e096.
- 817 71. Knoll AH, Grotzinger JP, Kaufman AJ, Kolosov P. Integrated approaches to terminal
818 Proterozoic stratigraphy: an example from the Olenek Uplift, northeastern Siberia.
819 *Precambrian Research*. 1995 May 1;73(1):251–70.
- 820 72. Pelechaty SM, Grotzinger JP, Kashirtsev VA, Zhernovsky VP. Chemostratigraphic and
821 Sequence Stratigraphic Constraints on Vendian-Cambrian Basin Dynamics, Northeast
822 Siberian Craton. *The Journal of Geology*. 1996 Sep 1;104(5):543–63.
- 823 73. Nagovitsin KE, Rogov VI, Marusin VV, Karlova GA, Kolesnikov AV, Bykova NV, et al.
824 Revised Neoproterozoic and Terreneuvian stratigraphy of the Lena-Anabar Basin and
825 north-western slope of the Olenek Uplift, Siberian Platform. *Precambrian Research*. 2015
826 Nov 1;270:226–45.
- 827 74. Cui H, Grazhdankin DV, Xiao S, Peek S, Rogov VI, Bykova NV, et al. Redox-dependent
828 distribution of early macro-organisms: Evidence from the terminal Ediacaran Khatyspyt
829 Formation in Arctic Siberia. *Palaeogeography, Palaeoclimatology, Palaeoecology*. 2016
830 Nov 1;461:122–39.

- 831 75. Vishnevskaya IA, Letnikova EF, Vetrova NI, Kochnev BB, Dril SI. Chemostratigraphy
832 and detrital zircon geochronology of the Neoproterozoic Khorbusuonka Group, Olenek
833 Uplift, Northeastern Siberian platform. *Gondwana Research*. 2017 Nov 1;51:255–71.
- 834 76. Cui H, Xiao S, Cai Y, Peek S, Plummer RE, Kaufman AJ. Sedimentology and
835 chemostratigraphy of the terminal Ediacaran Dengying Formation at the Gaojiashan
836 section, South China. *Geological Magazine*. 2019 Nov;156(11):1924–48.
- 837 77. Evans SD, Gehling JG, Droser ML. Slime travelers: Early evidence of animal mobility and
838 feeding in an organic mat world. *Geobiology*. 2019;17(5):490–509.
- 839 78. Evans SD, Droser ML, Gehling JG. Highly regulated growth and development of the
840 Ediacara macrofossil *Dickinsonia costata*. *Plos One*. 2017;
- 841 79. Evans SD, Huang W, Gehling JG, Kisailus D, Droser ML. Stretched, mangled, and torn:
842 Responses of the Ediacaran fossil *Dickinsonia* to variable forces. *Geology*. 2019 Nov
843 1;47(11):1049–53.
- 844 80. Baddeley A, Rubak E, Turner R, Rubak E, Turner R. *Spatial Point Patterns : Methodology
845 and Applications with R*. Chapman and Hall/CRC; 2015.
- 846 81. Berman M. Testing for Spatial Association between a Point Process and Another
847 Stochastic Process. *Journal of the Royal Statistical Society: Series C (Applied Statistics)*.
848 1986;35(1):54–62.
- 849 82. Wiegand T, Moloney KA. Rings, circles, and null-models for point pattern analysis in
850 ecology. *Oikos*. 2004;104(2):209–29.
- 851 83. Wiegand T, Wiegand K, Getzin S. Analyzing the Spatial Structure of a Sri Lankan Tree
852 Species with Multiple Scales of Clustering. *Ecology*. 2007;88(12):3088–102.
- 853 84. Wiegand T, Kissling WD, Cipriotti PA, Aguiar MR. Extending point pattern analysis for
854 objects of finite size and irregular shape. *Journal of Ecology*. 2006;94(4):825–37.

- 855 85. Wiegand T, Moloney KA, Naves J, Knauer F. Finding the Missing Link between
856 Landscape Structure and Population Dynamics: A Spatially Explicit Perspective. *The*
857 *American Naturalist*. 1999 Dec 1;154(6):605–27.
- 858 86. Loosmore NB, Ford ED. Statistical Inference Using the G or K Point Pattern Spatial
859 Statistics. *Ecology*. 2006;87(8):1925–31.
- 860 87. Diggle PJ. *Statistical analysis of spatial point patterns*. 1983.
- 861 88. Levin SA. The Problem of Pattern and Scale in Ecology: The Robert H. MacArthur Award
862 Lecture. *Ecology*. 1992;73(6):1943–67.
- 863 89. Besag J. Spatial Interaction and the Statistical Analysis of Lattice Systems. *Journal of the*
864 *Royal Statistical Society: Series B (Methodological)*. 1974;36(2):192–225.
- 865 90. Fraley C, Raftery AE. MCLUST Version 3 for R: Normal Mixture Modeling and Model-
866 Based Clustering*. 2017;57.
- 867 91. Grabarnik P, Myllymäki M, Stoyan D. Correct testing of mark independence for marked
868 point patterns. *Ecological Modelling*. 2011 Dec 10;222(23):3888–94.
- 869 92. Fraley C, Raftery AE. Bayesian Regularization for Normal Mixture Estimation and Model-
870 Based Clustering. *Journal of Classification*. 2007;24(2):155–81.
- 871 93. Péliissier R, Goreaud F. A practical approach to the study of spatial structure in simple cases
872 of heterogeneous vegetation. *Journal of Vegetation Science*. 2001;12(1):99–108.
- 873 94. Chiu SN, Stoyan D, Kendall JM. *Stochastic Geometry and Its Applications*. 2013.
- 874 95. Soznov NG, Bobkov NI, Mitchell EG, Kolesnikov A V, Grazhdankin DV. The ecology of
875 *Dickinsonia* on tidal flats. *IMECT 2019*. 2019;
- 876 96. Ivantsov AYu. Trace fossils of precambrian metazoans “Vendobionta” and “Mollusks”.
877 *Stratigr Geol Correl*. 2013 May 1;21(3):252–64.
- 878 97. Ivantsov AYu. Feeding traces of proarticulata—the Vendian metazoa. *Paleontol J*. 2011
879 May 1;45(3):237–48.

- 880 98. Ivantsov AYu. New reconstruction of Kimberella, problematic Vendian metazoan.
881 Paleontol J. 2009 Dec 14;43(6):601.
- 882 99. Ivantsov A.yu., Malakhovskaya Ya.e. Giant traces of vendian animals. DOKLADY
883 EARTH SCIENCES. 2002;385(6):618–22.
- 884 100. Managano MG, Buatois LA. The Cambrian revolutions: Trace-fossil record, timing,
885 links and geobiological impact. Earth-Science Reviews. 2017 Oct 1;173:96–108.
- 886 101. Hua H, Pratt BR, Zhang L-Y. Borings in Cloudina Shells: Complex Predator-Prey
887 Dynamics in the Terminal Neoproterozoic. PALAIOS. 2003;18(4–5):454–9.
- 888 102. Giangrande A, Geraci S, Belmonte G. Life-cycle and life-history diversity in marine
889 invertebrates and the implications in community dynamics. Oceanographic Literature
890 Review. 1995;8(42):662.
- 891 103. Liu AG, Mcilroy D, Antcliffe JB, Brasier MD. Effaced preservation in the Ediacara
892 biota and its implications for the early microfossil record. Palaeontology. 2011;54(3):607–
893 30.
- 894 104. Droser ML, Gehling JG. Synchronous Aggregate Growth in an Abundant New
895 Ediacaran Tubular Organism. Science. 2008 Mar 21;319(5870):1660–2.
- 896 105. Darroch SAF, Laflamme M, Clapham ME. Population structure of the oldest known
897 macroscopic communities from Mistaken Point, Newfoundland. Paleobiology.
898 2013;39(4):591–608.
- 899 106. Muscente AD, Bykova N, Boag TH, Buatois LA, Mángano MG, Eleish A, et al.
900 Ediacaran biozones identified with network analysis provide evidence for pulsed
901 extinctions of early complex life. Nat Commun [Internet]. 2019 Feb 22 [cited 2019 Oct
902 14];10. Available from: <https://www.ncbi.nlm.nih.gov/pmc/articles/PMC6384941/>
- 903 107. Grazhdankin DV, Balthasar U, Nagovitsin KE, Kochnev BB. Carbonate-hosted
904 Avalon-type fossils in arctic Siberia. Geology. 2008;36(10):803–6.

- 905 108. Reid LM, Holmes JD, Payne JL, García-Bellido DC, Jago JB. Taxa, turnover and
906 taphofacies: a preliminary analysis of facies-assemblage relationships in the Ediacara
907 Member (Flinders Ranges, South Australia). *Australian Journal of Earth Sciences*. 2018
908 Sep 25;0(0):1–10.
- 909 109. Ben-Hur E, Kadmon R. Heterogeneity–diversity relationships in sessile organisms: a
910 unified framework. *Ecology Letters* [Internet]. [cited 2019 Nov 13];n/a(n/a). Available
911 from: <https://onlinelibrary.wiley.com/doi/abs/10.1111/ele.13418>
- 912 110. Levin LA, Sibuet M, Gooday AJ, Smith CR, Vanreusel A. The roles of habitat
913 heterogeneity in generating and maintaining biodiversity on continental margins: an
914 introduction. *Marine Ecology*. 2010;31(1):1–5.
- 915 111. Vanreusel A, Fonseca G, Danovaro R, Silva MCD, Esteves AM, Ferrero T, et al. The
916 contribution of deep-sea macrohabitat heterogeneity to global nematode diversity. *Marine
917 Ecology*. 2010;31(1):6–20.
- 918 112. McClain C, Barry JP. Habitat heterogeneity, disturbance, and productivity work in
919 concert to regulate biodiversity in deep submarine canyons. *Ecology*. 2010;91(4):964–76.
- 920 113. Sommer S, Pfannkuche O. Metazoan meiofauna of the deep Arabian Sea: standing
921 stocks, size spectra and regional variability in relation to monsoon induced enhanced
922 sedimentation regimes of particulate organic matter. *Deep Sea Research Part II: Topical
923 Studies in Oceanography*. 2000 Jan 1;47(14):2957–77.
- 924 114. Leduc D, Rowden AA, Probert PK, Pilditch CA, Nodder SD, Vanreusel A, et al. Further
925 evidence for the effect of particle-size diversity on deep-sea benthic biodiversity. *Deep Sea
926 Research Part I: Oceanographic Research Papers*. 2012 May 1;63:164–9.
- 927 115. Monteiro PMS, Nelson G, van der Plas A, Mabile E, Bailey GW, Klingelhoeffer E.
928 Internal tide—shelf topography interactions as a forcing factor governing the large-scale

- 929 distribution and burial fluxes of particulate organic matter (POM) in the Benguela
930 upwelling system. *Continental Shelf Research*. 2005 Sep 1;25(15):1864–76.
- 931 116. Manno C, Stowasser G, Enderlein P, Fielding S, Tarling GA. The contribution of
932 zooplankton faecal pellets to deep carbon transport in the Scotia Sea (Southern Ocean).
933 *Biogeosciences*. 2015 Mar 25;12:1955–65.
- 934 117. Davison PC, Checkley DM, Koslow JA, Barlow J. Carbon export mediated by
935 mesopelagic fishes in the northeast Pacific Ocean. *Progress in Oceanography*. 2013 Sep
936 1;116:14–30.
- 937 118. Giering SLC, Sanders R, Lampitt RS, Anderson TR, Tamburini C, Boutrif M, et al.
938 Reconciliation of the carbon budget in the ocean’s twilight zone. *Nature*. 2014
939 Mar;507(7493):480–3.
- 940 119. Butterfield NJ. Plankton ecology and the Proterozoic-Phanerozoic transition.
941 *Paleobiology*. 1997;23(2):247–62.
- 942